DOI: 10.48011/asba.v2i1.1211

Phenomena Analysis of Ferroresonance and Self-Excitation in Subsea Power Systems ⋆

Diego de S. de Oliveira * **Gustavo Cezimbra B. Leal** *
João Adolpho V. da Costa * **Emanuel L. van Emmerik** *
Mauricio Aredes *

* *Instituto Alberto Luiz Coimbra de Pós Graduação e Pesquisa de Engenharia, Universidade Federal do Rio de Janeiro, UFRJ, (e-mails: diegosouza@lemt.ufrj.br, gustavoleal@lemt.ufrj.br, joao@lemt.ufrj.br, emmerik@lemt.ufrj.br, aredes@lemt.ufrj.br).*

Abstract: This article addresses the study regarding the emergence of ferroresonance and self-excitation phenomena in Subsea Power Systems - SPS, composed essentially of synchronous generators installed on a platform (Topside), a three-phase umbilical cable and the electrical loads, the latter constituted by induction machines located on the seabed and connected to the umbilical through a power transformer and power electronic converters. Such phenomena are conceptually stated and characterized in the scope of SPS and the simulations are carried out in the PSCAD/EMTDC software, in its parallel processing environment, to verify indications of the existence of problems in the base network of the subsea distribution system.

Keywords: Power Systems; Cables; Ferroresonance; Self-excitation; Subsea Power System.

1. INTRODUCTION

New equipment and marine electrical components have been announced by manufacturers for application in oil extraction in deep waters. The certification of this equipment by the companies involved in the oil extraction process is an extensive task, until the required reliability for the use of these new technologies in the exploration, extraction and production areas of the companies is achieved.

The level of detail in the SPS modeling required for this work will certainly subsidize companies to take on the greater challenge of equipment and control systems marinization for the most diverse elements used in this activity, such as cables, transformers, electrical machines and power converters, the latter used in the Variable Speed Drive (VSD) of subsea engines. This will contribute widely to a greater understanding of resonance and harmonic propagation problems in umbilical cables, in addition to the improvement of dc-links in specific applications at ultra deep water for the oil industry. These latter subjects are part of a single set and will be addressed in other two that, together with the present paper, are submitted for appreciation by the CBA2020 committee. They are: "DC-link project applied to Variable Speed Drives in Subsea Power Systems" and "Comparative Study of Technologies for Harmonic Propagation Mitigation in Subsea Power Systems".

Electrical machines, reactors and transformers are built with ferromagnetic materials. The nonlinear characteristics of these materials, such as saturation and hysteresis, can excite phenomena of ferroresonance, self-excitation or electromagnetic resonances, especially in a scenario of a power system composed of an expressive number of nonlinear charges.

The rest of this paper is organized as follows. Section 2 presents details of the adopted Subsea Power System (SPS) model. Section 3 introduces the ferroresonance concept and presents several configurations in which the SPS would be subjected to the phenomena. In Section 4, the self-excitation theory is analytically described and contains a simulation that is carried out in a test system using PSCAD/EMTDC electromagnetic transient program. Each of these sections conveniently has its own subsection of partial conclusions. Finally, this article is concluded by remarks in Section 5.

2. THE SUBSEA POWER SYSTEM

The adopted Subsea Power System (SPS) model for simulation, to analyze the aforementioned phenomena, is basically composed of a topside platform whose major component is the synchronous generator, a three-phase system named umbilical cable, transformers and power loads. All these elements will be depicted in the next sections.

2.1 Device Modeling

The entire SPS modeling and simulation procedures were performed through the PSCAD/EMTDC interface

⋆ This work was fully financed by Petrobras, through the Foundation for the Coordination of Projects, Research and Technological Studies - COPPETEC. In addition, was supported in part by the Coordenacão de Aperfeiçoamento de Pessoal de Nível Superior (Capes) and in part by the Conselho National de Desenvolvimento Científico (CNPq). The authors are with the Laboratory of Power Electronics and Medium Voltage Applications, Electrical Engineering Department, Instituto Alberto Luiz Coimbra de Pesquisa e Pós Grduação em Engenharia/Universidade Federal do Rio de Janeiro (COPPE/UFRJ), Centro de Tecnologia, Av. Athos da Silveira Ramos, 149, Ilha do Fundão, Rio de Janeiro - RJ

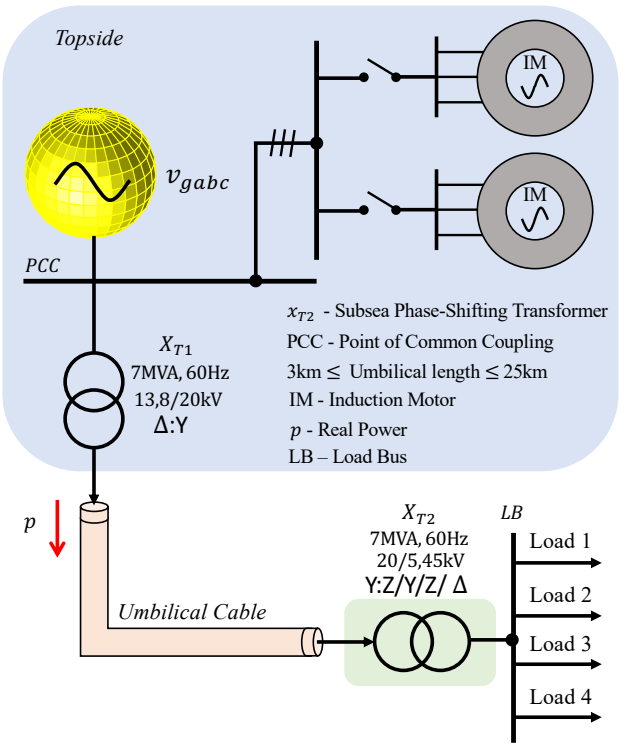

Figure 1. Subsea Power System representation

to Python by the respective Automation Library. This Python-PSCAD interface allows to automate several factors within a simulation. Although was recently launched and is only available for the current version, it proved to be extremely versatile and was essential for automatic simulations of so many cases and with reduced computational burden. The simulation is performed with the SPS divided into five sub-modules and these five sub-systems were simulated in an environment with five processing units.

Topside

The generator representation shown in Figure 1 consists of a three synchronous generator equivalent, each one with a 31.25 MVA power rating, that have been simulated coherently in order to speed up the simulations, justified by the fact that inter-machine dynamics are not the focus of this research. Other electric devices are two directly grid-connected Induction Motors (IM). The latter is lumped, intended to represent the sum of all the other directly grid-connected motors. The first is the biggest directly connected motor, compressor, at topside. Both will be appropriately addressed in the *Load* section.

The synchronous generator model was achieved using the advanced options included in this PSCAD component for modeling a synchronous machine, such as the interface to excitation system, which in this work was adopted the IEEE type Alternator Supplied Rectifier Excitation System (AC1A) recommended in IEEE Std (2016), and to start-up and initialization features according IEEE Report (1973). The mechanical interaction with the turbines is modeled with the following control blocks: three real poles in series, a reference for speed and one for power.

Umbilical Cable

In addition to serving as a pipeline for chemicals used in oil extraction, the umbilical's electric vein, commonly known as umbilical cable, consists of a main three-phase structure composed of three coaxial single-phase cables, and radially disposed, contains insulating material layers, metallic shielding and semiconductor material layers. Depending on the application, the metallic shield can be grounded at one or both ends, or be isolated throughout its end.

In summary, the modeling of the coaxial cable was carried out by comparing the simulated results with the actual parameters provided by the manufacturer's datasheet. For this, two strategies were used, the first of which uses the routine of calculating line parameters based on the cable geometry and constituent material, known as Line Constants Program (LCP). The second strategy is based on directly entering data provided by manufacturers, this is known as *Manual Data Entry*. Both routines have advantages and disadvantages, and the one with the lowest percentage difference from the manufacturer's data was adopted.

The cable is modeled with distributed traveling wave model and, given the need for investigations involving harmonic propagation (as can be seen in papers related in the Introduction) with frequency-dependent model, is the preferred model due to be numerically robust and more accurate than any other commercially available. The representation of the geometry and material characteristics is shown in Table 1, in which SL and NS mean Semiconductor Layer and Not Specified, respectively.

Table 1. Constructive characteristics of the umbilical cable.

Layer	Thickness (mm)	ρ(Ω.m)	ε_r	μ_r
Main conductor	9.1	17.2×10^{-9}	NS	1
First SL	1.0	NS	NS	1.0
Main insulation	4.0	NS	2.8	1.7
Second SL	1.0	NS	NS	1.0
Metal Shield	3.5	17.2×10^{-9}	NS	1.0
Outer insulation	1.5	NS	2.8	1.0

The soil was modeled with a resistance of 0.01 Ω/meter. This value seeks to simulate a cable submerged in salt water and is based on Anderson (1995). In some situations, depending on the thickness and conductivity of the metallic shield, the influence of the ground becomes negligible even at low frequencies (Ametani et al., 2015).

Transformer

The modeled system is a SPS intended to supply subsea loads whose core part consists of induction motors, acting as a traction element for subsea pumps, as will be detailed in the next subsection. The machine is controlled by a back-to-back converter, in which the grid voltage is rectified, feeding a dc-link. The rectifier in question is composed of a three-phase diode-bridge, which produces harmonics in the current of order $6n\pm1$, which deteriorates the quality of energy coming from topside. This can cause unforeseen problems in the cable, since its behavior is not the same as conventional transmission lines (high capacitance).

The solution to this inconvenience is the multi-pulse converter (Paice, 1996). In this topology, the phase-shifting transformer becomes indispensable, since it allows the achievement of a desired lag between the grid voltages and the input voltages of the converter terminals, electrical insulation and correct voltage levels in its secondary. This is a usual technique for eliminating harmonics (Wu and Narimani, 2017), minimizing the need for additional filters, which is especially desired in subsea applications.

In this context, the topside transformer is conventionally a three-phase transformer with the sole function of transporting power at a higher voltage level than the generator voltage. On the other hand, the subsea transformer, in addition to providing an appropriate voltage level to the rectifier and also providing electrical insulation between the rectifier and the network, has the main role of canceling specific harmonics (Wen et al., 2012). For this, the X_{T2} transformer in Figure 1 represents one three-phase transformer, feeding the four loads, with different phase-shifting between the voltages of the primary winding and the four respective secondary winding connections. In this way, a phase-shifting transformer was modeled with the primary winding in the isolated Y connection and the secondary with connections in Zig-Zag, isolated Y connection and Δ so that the phase shifts of $-15°$, $0°$, $15°$ and $30°$ were obtained.

Loads

The loads used for the SPS studies all consist of three-phase Induction Machines (IM). The first of the two induction motors positioned on the topside is an 11 MW compressor corresponding to the largest power load on the platform, and a second IM, named Lump load is the configuration resulting from the grouping of all loads on the platform, except for the largest motor previously mentioned. The rated values of the Lump load are shown in Table 2.

Table 2. Rated values for lumped load.

Parameter	Value
Voltage	13.8 kV
Power capacity	50 MW
Power factor	0.85

The remaining four loads are subsea IM, installed at a depth of 3 km and a total distance up to 25km from topside. The motors are of the SESP type (Subsea Electrical Submersible Pump) and are mechanically coupled to hydraulic pumps to lift the fluids from the oil reservoir, through the producing well, to the surface treatment unit. They are driven by power electronics converters and the mechanical torque imposed by the load was represented by a quadratic dependence on the rotational speed, as in centrifugal pumps (Stephan, 2013), multiplied by the factor 0.73.

Two converters in the back-to-back configuration make the electrical interface between the network and the SESP, as shown in Figure 2. A single line commuted converter plays the role of rectifier, injecting power into a capacitive dc-link. An IGBT controlled converter acts as an inverter in order to perform the IM speed control (Mohan et al., 2003). For this, the simple control strategy is to maintain

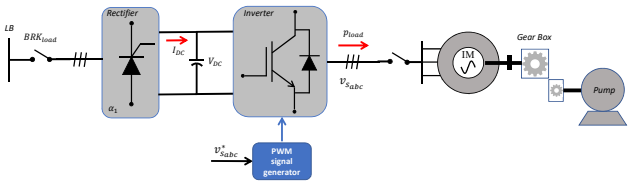

Figure 2. Subsea power load representation

the scalar V/f constant in open loop, due to the adopted hypothesis that there is no information from speed, voltage and/or current sensors, which contributes to the reliability and robustness of the whole system. This control technique is based on the simplified, steady-state model of the induction machine and allows speed control by keeping the air gap flow constant. This can be approximated by the magnitude of the stator voltage divided by the angular frequency (rad/s) after some simplifications have been made (Chapman, 2013)(Leonhard, 2001).

3. FERRORESONANCE

Ferroresonance is a specific concept of the resonance phenomenon, which originates from the concept of resonant circuits, where the inductive and capacitive reactance values match for a given frequency, in which the undesirable presence of overcurrents and/or overvoltages is observed (Bethenod, 1907). It is characterized as an electromagnetic resonance phenomenon that is established in the presence of a non-linear inductance, such as the representative inductance of the transformer cores, whose reactance depends not only on the frequency, but also on the magnetic flux density in the ferromagnetic core (Valverde et al., 2007). The concept of ferroresonance was first addressed in literature in 1920 (Boucherot, 1920), where it is described as a group of phenomena of an oscillatory nature that may be present in configurations composed, at least, by a voltage source, a non-linear inductance, reduced ohmic losses and significant capacitance.

In other words, a real power system is subject to the occurrence of ferroresonance as long as there is a series association between the non-linear inductance of the transformer and a capacitive element. Significant capacitance values are found in cables or transmission lines connected to the transformer (Butler and Concordia, 1937). Total capacitance can also receive the contribution, although to a lesser extent, of elements such as potential transformers and circuit breakers. The capacitance values present in such devices are significantly lower than those found in the transmission system and, therefore, will not be considered in this work.

3.1 Theoretical Framework

A real power system is subject to the occurrence of ferroresonance as long as there is a series association between the non-linear inductance of the transformer and a capacitive element, the latter being from the transmission line or cable connected to the transformer. In the case of the subsea cable, object of this work, the capacitance can be self-capacitance X_{cp}, due to the capacitive effect established between each of the phases and the metallic shield, or even the mutual capacitance between phases

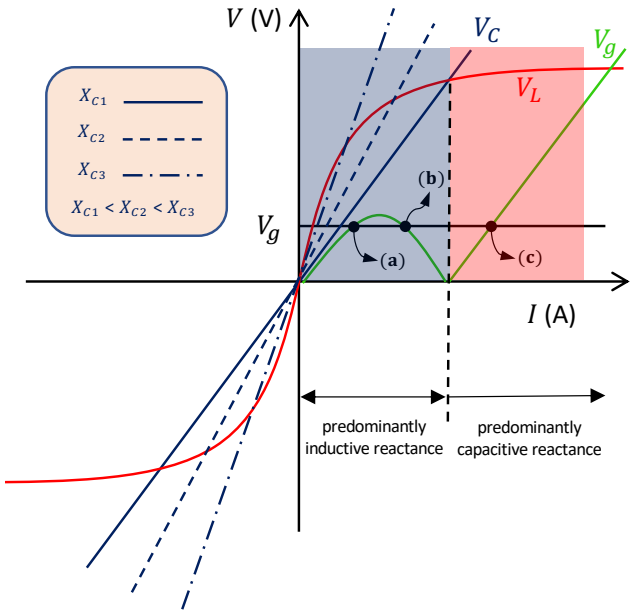

Figure 3. Graphical approach for ferroresonance evolution effect according to cable capacitance changes.

X_{cm}. The X_{cp} and X_{cm} reactance must be observed in each of the cases discussed in the following subsections.

Figure 3 provides a graphical approach to the series ferroresonance, such behavior is described in (1), where L is given qualitatively by a direct function of current $L(\dot{I})$.

$$\dot{V_g} = j\left(\omega L\left(\dot{I}\right) - \frac{\dot{I}}{\omega C}\right) \tag{1}$$

From the voltage characteristics is observed that the multiple possible points of operation in the SPS can be fundamentally a function of the capacitance of the umbilical cable and, therefore, of the cable length. Those points can be obtained from the slope of the graph corresponding to V_C. Two well-defined operating regions can also be seen for the resulting predominantly inductive reactance, where the non-ferroresonant linear operating region (linear L) is contained, and the resulting capacitive situation, the region containing the unstable operating point (saturated L). The border between those regions is given by the current value at which the topside voltage is null, which occurs when the magnetization curve of the transformer iron core intercepts the capacitance voltage.

The three operation points depicted in Figure 3 can be briefly explained as follows (Greenwood, 1991):

- Point (a): stable operating point. Linear zone of L that would not lead SPS to a ferroresonance situation.
- Point (b): unstable operation point. Any incremental change in current will cause changes in inductive and capacitive voltages such that will not lead the current to return to its initial value.
- Point (c): stable operation point, however, its a saturation region that brings the SPS to the ferroresonance condition.

In this context, in three-phase distribution systems, the appearance of the phenomenon is associated with some factors and conditions such as the constructive characteristic of the transformer core, the load connected to the secondary of the transformer and the length of the cable/line. However, it will also be conditioned to some specific configurations whose occurrence is directly related to transitory situations (Hopkinson, 1965), resulting from contingencies in the system, such as overvoltages due to lightning strikes, energizing or removing loads, occurrence or elimination of faults (Viena, 2010).

The Figure 1 illustrates the SPS with emphasis on the elements of the system that deserve attention with regard to the ferroresonance phenomenon. The highlights are the types of grounding of the synchronous generator (source of the SPS) and the type of connection of the phase-shifting transformer, to which the non-linear inductance is attributed (IEEE Std, 1978). The step up transformer located at topside, given its Delta-isolated star connection, does not contribute to the characterization of the resonant series-association, that is, it does not establish a path to earth and, therefore, it is only considered as an inductance in series with the umbilical.

3.2 Possible system configurations

In the following sections, all possible specific configurations of the SPS that could lead the system to a ferroresonance situation will be presented.

Monopolar transformer closure with primary configured in grounded star

In this and the next items, the transformer in question consists of the phase-shifting transformer and the switching operation occurs at the origin of the system (topside). Figure 4 illustrates the situation in which the closing of one of the phases takes place, with the generator grounded, the transformer connected to a grounded star, and the umbilical without connection to the earth, together with the respective established equivalent resonant circuit.

In this case, the conditions for resonance are fully met. It is important to repeat that, for this situation to occur, it is necessary that the primary of the phase-shifting transformer is connected in star with a grounded neutral and that, simultaneously, there is a failure in the insulation of the generator neutral, since it is grounded through a high impedance. Since monopolar switching is a necessary condition, and normal switching is three-phase, a mono- or bipolar switching fault has to occur to favour ferroresonance.

Monopolar transformer closure with primary configured in isolated star

For this situation, in addition to the need for insulation failure in the generator ground, in order to establish a resonance path between the capacitance of the phases kept open (in this case, phases a and b) and the cable armature, and inductance of the phase-shifting transformer, it is necessary also that the cable armor is grounded at one or more points along its length. Figure 5 illustrates the described situation. By direct observation of Figure 5, the current's path at the moment of closing phase c illustrates

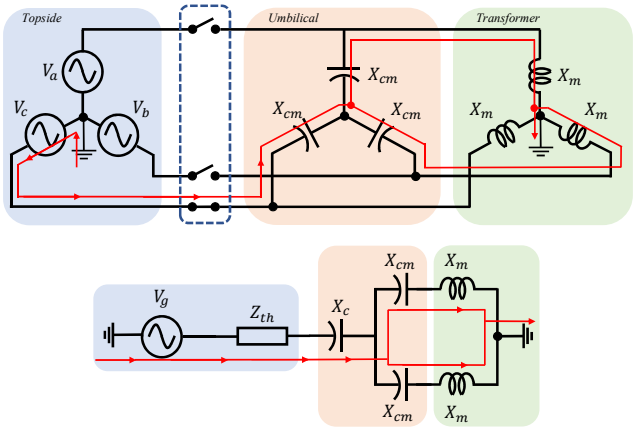

Figure 4. Monopolar closing configuration - grounded Y.

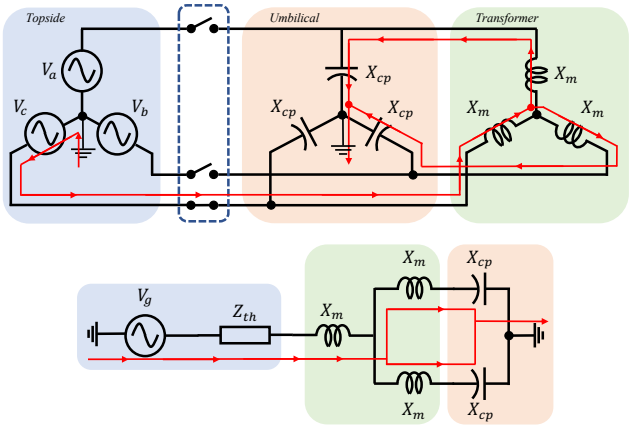

Figure 5. Monopolar closure configuration - isolated Y.

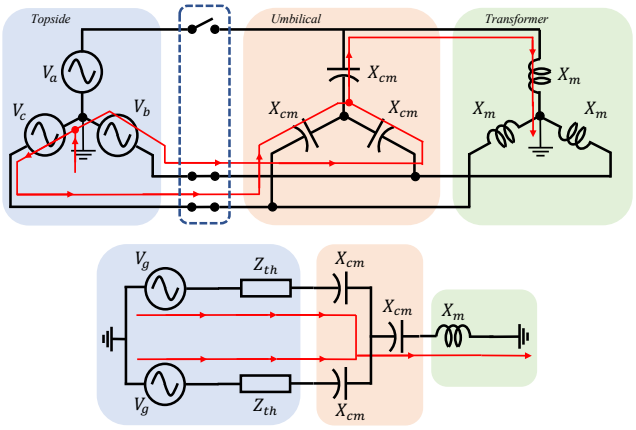

Figure 6. Bipolar closure configuration - grounded Y.

that the capacitance that contributes to the LC-circuit corresponds to the capacitance of the phases that remained open.

Bipolar transformer closure with primary configured in grounded star

The situation shown in Figure 6 denotes the resonant path formed by the capacitance related to the three phases of the umbilical cable with the inductance of the phase-shifting transformer belonging to the phases that underwent the switching maneuver.

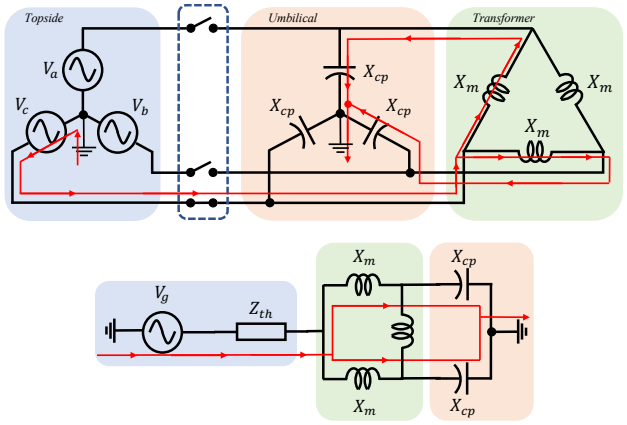

Figure 7. Monopolar closing configuration - Delta.

In addition to the these configurations, there may also be two cases in which the phase-shifting transformer (on the subsea) has its primary winding connected in delta. In this case, for there to be a resonant circuit, two conditions must necessarily occur simultaneously: failure of the generator insulation and the umbilical cable armature must be grounded. Such scenarios are shown in Figure 7 and in Figure 8 and their respective equivalents.

The analysis of the scenarios set out above shows that in all of the aforementioned situations, there is a need for a failure in the generator grounding system. In addition, in all situations it is necessary to have a failure in the switching maneuver which, normally, is three-phase. In cases where the path is through the capacitance between phase and armature, the armature would necessarily have to have at least one grounding point. In this context, the umbilical's data-sheet mentions the grounding of the armature at both ends.

3.3 Partial Conclusion

Finally, it is important to note that both umbilical capacitance values, specific to each phase and mutual between phases, must be observed in the ferroresonance phenomenon. In cases where the phase-shifting transformer does not offer a path to earth, cases represented by Figure 5, Figure 7 and in Figure 8, the phase-to-ground capacitance must be higher than the mutual one. This will cause the phase-to-ground capacitive reactance to be lower ($X_{cp} < X_{cm}$), thus offering a lower impedance path and causing a greater portion of the current to circulate to the earth, forming the resonant circuit. For the cases in which the primary winding of the phase-shifting transformer is connected to a grounded star, it is necessary that the mutual capacitance value is higher so that, in this way, the phase-to-phase capacitive reactance is lower ($X_{cm} < X_{cp}$) and the path of least impedance is established between phases. Therefore, after traversing the cable mutual capacitance, the current will flow to the earth through the transformer's grounding, a situation represented by Figure 4 and Figure 6.

4. SELF-EXCITATION

In this section, the phenomenon of self-excitation in synchronous generators is characterized within the scope of a

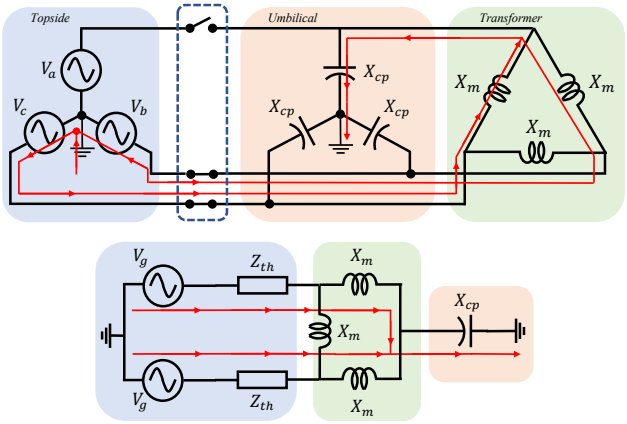

Figure 8. Bipolar closing configuration - Delta.

SPS. The focus is on the theoretical configurations that can lead the generators, located on the platform, to the emergence of overvoltages related to predominantly capacitive loads connected to its terminals.

Self-excitation in synchronous machines is a condition of instability associated with increased magnetic field in the main poles, being characterized mainly by the rapid increase in voltage at the machine terminals due to the appearance of a predominant capacitive load connected to its terminals. In power systems, the appearance of capacitive load is related to specific contingency situations in the system, such as load rejection in long trunks of alternating current transmission and in direct connections to capacitive banks (of filters and/or reactive support) in case of pole blocking of HVDC-transmission links. In this context, considering that HVDC transmission system is outside the scope of this article, the possibility of the emergence of self-excitation is therefore restricted to a single emergency condition, that is, a severe load rejection when SPS are under normal operating conditions. This situation results from an opening maneuver of the three-pole sectioning represented by BRK_{LOAD} in Figure 2, resulting in the occurrence of a complete load rejection, in which the synchronous generator remains connected to the umbilical with the terminal open (Portugal, 2007).

4.1 Analytic Approach

Capacitive current I_{cap} from the capacitance of the cable contribute to the rapid growth of the main field, an increase that is characterized by overvoltages at the generator terminals. For the purpose of simplifying calculations, much of the available literature on self-excitation does not consider the sub-transitory effects of the synchronous machine rotor. From the equations of the synchronous machine model for stability studies, in which the leakage magnetic flux, voltages and currents are represented on the dq reference, presents a complete mathematical development of the phenomenon of self-excitation, carried out by including the equivalent capacitance seen from the terminals of the synchronous machine in the voltage equations for d and q axes (Portugal, 2007) (Saccomanno, 2003).

From the analysis in the frequency domain of these results with direct observation of the root locus of the characteristic equation in reference dq, varying X_C in the range of 0 to ∞, one concludes for the d axis, that the self-excitation region occurs for values of X_C within the interval between X_d and $X_d^{''}$ and, for the q axis, that the self-excitation region occurs for values of X_C within the interval between X_q and $X_q^{''}$. It is important to highlight that the leakage reactance of the topside transformer must be added to the unsaturated reactance. This total reactance, X_T, is 2.7205 Ω. From this, it is concluded that the conditions (2), (3), (4) and (5) must be respected so that a situation of instability does not occur. This is graphically summarized in Figure 9, which illustrates this behavior for the d and q axes, where ω is the electrical angular speed, and, L and ψ_s are inductance and stator flux leakage, respectively.

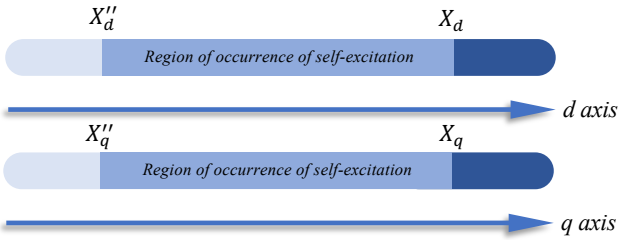

Figure 9. Self-excitation regions in dq reference.

$$\frac{1}{\omega C} \notin [\omega L_d'', \omega L_d] \tag{2}$$

$$\frac{1}{\omega C} \notin [\omega L_q'', \omega L_q] \tag{3}$$

$$\frac{\mathrm{d}\psi_{sd}}{\mathrm{d}i_d} < \frac{1}{\omega^2 C} \tag{4}$$

$$\frac{\mathrm{d}\psi_{sq}}{\mathrm{d}i_q} < \frac{1}{\omega^2 C} \tag{5}$$

Table 3. Reactance values of the synchronous machine.

Unsaturated reactance values	X_{pu}	X_Ω
d-axis reactance (X_d)	1.1693	2.3752
Sub-transitory d-axis reactance ($X_d^{''}$)	0.1	0.2031
q-axis reactance (X_q)	1.1479	2.3317
Sub-transitory q-axis reactance ($X_q^{''}$)	0.2	0.4062

In Table 4, the reactance $X_{T\Omega}$ corresponds to the steady-state reactance and sub-transient reactance in the dq-reference of the synchronous machine (Table 3), in Ohm, added to the leakage reactance of the topside transformer.

Table 4. Corrected reactance values of the synchronous machine.

Unsaturated reactance values	$X_{T\Omega}$
d-axis reactance (X_{dT})	5.0957
Sub-transitory d-axis reactance ($X_{dT}^{''}$)	2.9236
q-axis reactance (X_{qT})	5.0522
Sub-transitory q-axis reactance ($X_{qT}^{''}$)	3.1267

According to (6), longer cables correspond to higher capacitance and, therefore, lower self and mutual admittance, and given that, the studied base system contains the

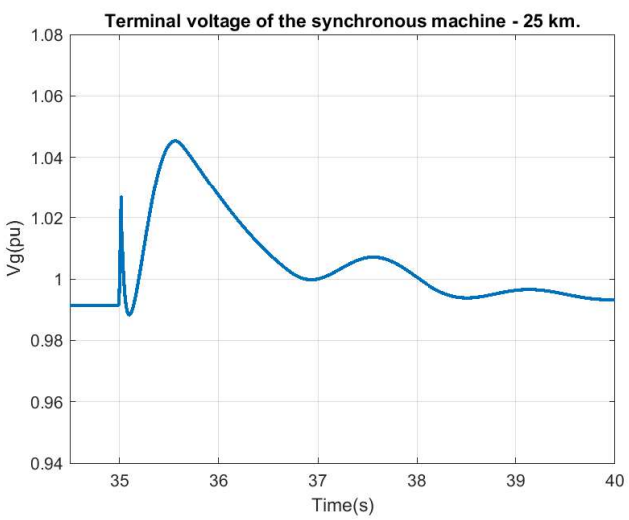

Figure 10. Overvoltage caused by full load rejection.

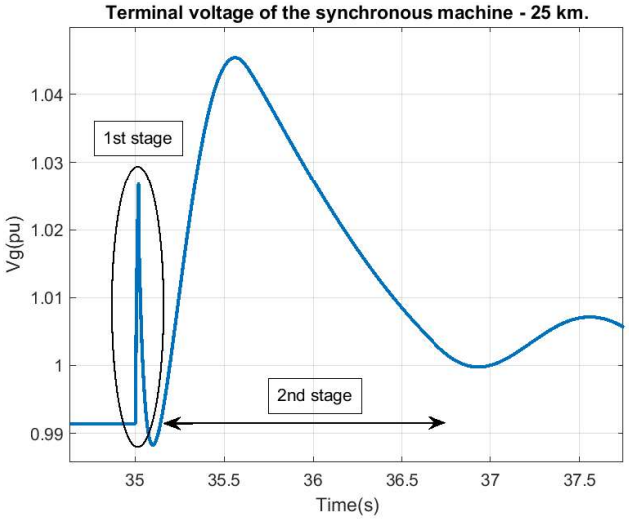

Figure 11. Detailed typical form of overvoltage.

largest length of umbilical, 25 km. This length is the one that is closest to the limit of the region of instability (X_d and X_q). In C_p equation, r and GMD (geometric mean distance) are the radius of each conductor and equivalent conductor spacing, respectively (Grainger and Stevenson, 1994). This latter, is the cube root of the product of the three-phase spacing, which in such umbilical, are equivalent.

$$C_p = \frac{2\pi\varepsilon_0}{\ln \frac{GMD}{r}} \text{F/m} \tag{6}$$

From those generator parameters and having the capacitive reactance of umbilical at fundamental frequency, which is equivalent to $X_c = 7.06081 \times 10^6$ Ω.m, it can be concluded that X_c is greater than the upper limit of the region of instability and self-excitation is then determined by the following conditions in the dq reference:

$$X_d^{''} < X_d \ll X_c$$
$$X_q^{''} < X_q \ll X_c$$

4.2 Parametric Analysis

Figure 10 illustrates the behavior of the overvoltage resulting from a full load rejection occurred at time $t = 35$ s for length 25 km, after a long time operating in steady state. At Figure 11 a sudden increase in V_g in the first two cycles after event can be observed, however, not exceeding 5% of nominal voltage.

The figure highlights a detail of the typical V_g voltage profile after the load rejection in which two critical stages are observed. The first stage occurs immediately after time $t = 35$ s, featuring a sudden unsustainable rise in voltage that lasts less than two cycles of the fundamental frequency, a fact that reinforces the need for the phenomenon to be analyzed with the help of an electromagnetic transient tool. The second stage, which is more harmful to the elements of the system, is characterized by a sustained rise in voltage. This behavior depends fundamentally on the magnetic flux of the synchronous machine and on the dynamics of the voltage regulators (Farias and Jovita, 2001), hence the importance of a detailed modeling, as depicted in Section 2.1.

4.3 Partial Conclusion

It can be concluded that, for lengths of umbilical cable characteristic of a realistic subsea distribution system, the overvoltages at the terminals of the synchronous machine resulting from the phenomenon of self-excitation caused by load rejection does not characterize a problem for the studied scenario, in view of the low characteristic capacitance values of the umbilical cable. In this context, for the phenomenon to occur, lengths of this umbilical cable greater than 1500km would be needed, which is unrealistic.

Studies also show that the self-excitation of the synchronous machine must be especially observed in subsea distribution systems, whose cable length or construction characteristics are such that it leads to situations in which the phenomenon is possible, which does not occur in the studied scenario. In other words, at the threshold of the emergence of self-excitation ($X_C \approx X_{dT}$ e $X_C \approx X_{qT}$), a situation of load rejection raises the frequency of the system, causing variation in both capacitive cable reactance (decrease) and internal reactance of the machine (increase). The load-generation imbalance can cause X_C to temporarily fit into the critical region regarding the self-excitation.

Self-excitation is characterized by being a phenomenon of difficult equation to solve, given that it is strongly influenced not only by the non-linearity of the magnetization reactance of the topside and subsea transformers and the reactance of the machine at the instant of rejection, but also suffers the influence of umbilical cable parameters. It is evident that the worsening of self-excitation in three-phase umbilical cables with coaxial conductors grouped inside a pipeline as a result of capacitance is less likely to occur compared to long overhead transmission lines, since the self capacitance (between the conductor and the metallic armor) and the mutual is small because of the reduced separation distances between these elements. It is important to reiterate that the aspects of self-excitation

must be studied with an electromagnetic transient tool and with detailed modeling due to interference of the response dynamics of the excitation regulators and of the cable parameters.

5. CONCLUSION

Ferroresonance is an adverse condition due especially to the series association formed by the equivalent capacitance of the umbilical cable and the nonlinear inductance of the phase-shifting transformer, which can cause sustained overvoltages and overcurrents, damaging equipment. The self-excitation in synchronous machines is an electrical instability that is associated with increased main-flux links, being characterized mainly by the sudden increase in the terminal voltage of the machine, resulting from the capacitive element seen from the stator terminals. In this work, this capacitive effect is related to specific SPS configurations, in which there is a severe rejection of the underwater load associated with long umbilical lengths. Both phenomena may be quite complicated for analytical treatment because of the presence of hysteresis in the magnetic characteristic, since the high non-linear characteristic of the three or more transformer-core is preponderant to characterize them.

This paper is concerned to define those system characteristics and operating conditions that would conduct the system to risk of being under ferroresonance and self-excitation situations. In the ferroresonance analysis it can be seen that, for the phenomenon to occur in the base case of SPS, there must be a combination of factors such as failure in the isolation of the generator neutral, failure in the three-pole switching operation and, in addition, the umbilical cable armature must be grounded in at least one point. This last condition is necessary for the phenomenon to occur only if the primary winding of the phase-shifting transformer does not allow a path to earth, that is, if it is connected to an isolated star or delta. The appearance of overvoltages resulting from self-excitation is an inconvenience that must be avoided as it is highly harmful, especially in the scope of the isolation of high-cost equipment used in the oil extraction process. This work has the main purpose of supporting the project and expansion planning engineers of subsea power systems with elements that contribute to reduce or eliminate their probability of occurrence.

REFERENCES

Ametani, A., Ohno, T., and Nagaoka, N. (2015). *Cable system transients: Theory, modeling and simulation*. John Wiley & Sons.

Anderson, P.M. (1995). *Analysis of faulted power systems*, volume 445. IEEE press New York.

Bethenod, J. (1907). Sur le transformateur et résonance. *L'Éclairage électrique*, 53, 289–96.

Boucherot, P. (1920). Éxistence de deux régimes en ferrorésonance. *Rev. Gen. de L'Élec*, 8(24), 827–828.

Butler, J. and Concordia, C. (1937). Analysis of series capacitor application problems. *Electrical Engineering*, 56(8), 975–988.

Chapman, S.J. (2013). *Fundamentos de máquinas elétricas*. AMGH Editora.

Farias, A. and Jovita, R. (2001). Limitações operativas causadas por auto-excitação em máquinas síncronas. *XVI SNPTEE–XVI Seminário Nacional de Produção e Transmissão de Energia Elétrica, Campinas, SP*.

Grainger, J.J. and Stevenson, W.D. (1994). *Power system analysis*. McGraw-Hill.

Greenwood, A. (1991). Electrical transients in power systems.

Hopkinson, R.H. (1965). Ferroresonance during single-phase switching of 3-phase distribution transformer banks. *IEEE Transactions on power Apparatus and Systems*, 84(4), 289–293.

IEEE Report (1973). Dynamic models for steam and hydro turbines in power system studies. *IEEE Transactions on Power Apparatus and Systems*, PAS-92(6), 1904–1915.

IEEE Std (1978). Ieee guide for application of transformer connections in three-phase distribution systems. *ANSI/IEEE Std C57.105-1978*, 1–39.

IEEE Std (2016). Ieee recommended practice for excitation system models for power system stability studies. *IEEE Std 421.5-2016 (Revision of IEEE Std 421.5-2005)*, 1–207.

Leonhard, W. (2001). *Control of electrical drives*. Springer Science & Business Media.

Mohan, N., Undeland, T.M., and Robbins, W.P. (2003). *Power electronics: converters, applications, and design*. John wiley & sons.

Paice, D.A. (1996). *Power electronic converter harmonics: multipulse methods for clean power*. IEEE press.

Portugal, P.M.M. (2007). Análise de auto-excitação e curto-circuito capacitivo em geradores síncronos conectados a grandes sistemas de transmissão CCAT e CAAT. *Rio de Janeiro*.

Saccomanno, F. (2003). *Electric power systems: analysis and control*. Wiley-Interscience.

Stephan, R.M. (2013). Acionamento, comando e controle de máquinas elétricas. *Editora Ciência Moderna Ltda*.

Valverde, V., Mazón, A., Zamora, I., and Buigues, G. (2007). Ferroresonance in voltage transformers: Analysis and simulations. In *International Conference on Renewable Energies and Power Quality (ICREPQ" 07), Sevilla, Spain*, 465471.

Viena, L. (2010). *Modelagem de transformadores no programa ATP para o estudo do fenômeno da ferrorressonância*. Ph.D. thesis, Dissertação de Mestrado, UFBA.

Wen, J., Qin, H., Wang, S., and Zhou, B. (2012). Basic connections and strategies of isolated phase-shifting transformers for multipulse rectifiers: A review. In *2012 Asia-Pacific Symposium on Electromagnetic Compatibility*, 105–108. IEEE.

Wu, B. and Narimani, M. (2017). *High-power converters and AC drives*. John Wiley & Sons.